International Journal of Development Mathematics Vol 1 Issue 4 Page No. 099 - 111

INTERNATIONAL JOURNAL OF DEVELOPMENT MATHEMATICS

ISSN: 3026-8656 (Print) | 3026-8699 (Online)

journal homepage: https://ijdm.org.ng/index.php/Journals

Effects of Interfacial Parameters and Temperature on Effective Schottky Barrier Height of Metal-Wrapped (Al-Gan) Nanowire Schottky Diode

Dogari John[a], Usman Adam[b*] and Yerima Benson[b]

[a]Department of Science Laboratory Technology, Modibbo Adama University, Yola PMB 2076, Adamawa State, Nigeria

[b]Department of Physics, Modibbo Adama University, Yola PMB 2076, Adamawa State, Nigeria

ARTICLE INFO

Article history:
Received 11 September 2024
Received in revised form 15 November 2024
Accepted 29 November 2024

Keywords:
Effective Schottky barrier height, Interface parameters, Metal-Semiconductor junction, Nanowire, Temperature.

MSC 2020 Subject classification:
81Q37, 81V65, 82D77, 82D80

ABSTRACT

Junction interface parameters (interface states density, interface layer thickness, interface permittivity and neutral surface states) and temperature effects have been studied. Results have shown that for the scaled structure doping functions below degeneracy state and temperature have significant impact on the effective Schottky barrier height while the interface parameters show no significant change. The barrier height has been observed to increase as the temperature increases almost linearly by ~5.171×10-3eV with increase in temperature from 300K to 420 K and this may be associated with the avalanched charge carriers being transported across the barrier height. The interface layer thickness in the range of 1.5 nm to 3.0 nm shows no effect on the carrier transport characteristics curves of the Schottky diode whereas the ideality factor has been found to decrease with an increase in temperature.

1. Introduction

The operation of electronic devices such as field-effect transistors, solar cells and electroluminescent diodes is largely governed by the metal-semiconductor (M-S) interfaces where charge carriers are injected or extracted. The M-S interface can be classified into two types: Schottky and Ohmic (Rhodrick, 1978). If the transport of an electric current through a Schottky interface is hindered by the presence of an energy barrier height (Schottky barrier height, SBH), the current-voltage (*I-V*) characteristics display rectification behavior. On the other hand, Ohmic contacts possess (effectively) no energy barrier and their *I-V* characteristics obey Ohm's law. Because of their current rectifying behavior, Schottky-type M-S interfaces are employed as a basic active electronic component, called a Schottky diode (Calahorra and Ritter, 2013). The rectifying metal-semiconductor contact (Schottky diodes) is of interest for most elemental and compound semiconductors. In general, Schottky barrier diodes (SBDs) are considered as the least complex power device and are discussed as an alternative for p-n junctions (Rhodrick, 1978; Guven and Nazim, 2004). They have very fast switching times and work with only majority carriers (Rhodrick *et al*, 1993; Das *et al*., 2009). For a proper understanding of the electrical properties of any metal-semiconductor junction, it is important to know the contact behavior. The formation of Schottky barriers (SBs) at the metal-semiconductor interface has been a subject of debate for decades. Schottky and Mott proposed a model, in which the SB height equals to the difference between the work function of metal, and the electron affinity of the semiconductor. Then, a linear dependence should exist between the Schottky barrier height, and the metal work function. Corresponding to this, SB heights of various elemental metals, including Au, Ti, Pt, Ni, Cr, have been reported (Guven and Nazim, 2004). In these reports, SBH changes but do not scale proportionally with metal work functions. All of these junctions are axial M-S interfaced junctions and are either Three-dimensional (3D) or Two-dimensional (2D).

One-dimensional (1D) nanostructure represents the smallest dimension of structures that can efficiently transport charge carriers, and thus are ideally suited for the critical and ubiquitous task of moving and routing charges, which constitute information. They also exhibit critical device function, and thus can be exploited as both the wiring and device elements in future architecture for functional nano systems (Wolf, 2004).

* Corresponding author. Tel.: +2348034122680
E-mail address: auyaayyu@mau.edu.ng (Adam Usman.)
https://doi.org/10.62054/ijdm/0104.08

In this work, we carefully undertake a study on metal-wrapped semiconductor, Aluminum-Gallium nitrite (Al-GaN), a cylindrical nanowire Schottky junction, by considering the doping profile effect on the nanowire radii (GaN), interface parameters effect on the barrier height from the exact solution of metal-semiconductor interface. Also, the effect of the interface parameters on the carrier transport characteristics of the junction. In the continuous miniaturization of materials, unique properties that are different from those of their bulk counterparts result. At nano scale, the behavior of materials drastically get changed and hence their properties. Particularly in semiconductors, it results due to motion of electrons to a length scale range that is equal to or smaller than the length scale of the electron Bohr radius, $a_0 = 4\pi\hbar^2\varepsilon_0/q^2m^* = 0.0529$ nm, where $\hbar \equiv h/2\pi$ the reduced Plank's constant, ε_0 is the permittivity of free space, q is the electronic charge and m^* the effective mass of an electron. That is generally a few nanometers (Zettil, 2009). Electron transport is described classically by Boltzmann transport equation, which introduces mean-free-path, Λ. At a relatively low temperature, considerable contribution to conductivity, σ, is given to electrons with energy close to Fermi surface. Hence, conductivity is given by (James, D. P., and Bernard, C. B., 2007; and Tolley, R., 2013) as

$$\sigma = \frac{n q^2 \tau}{m^*} \tag{1}$$

where n is the concentration of the carrier, and τ is the relaxation time. It is an intrinsic property of the material that does not depend on the geometry of the material.

Another parameter characterizing the system is Fermi wavelength, $\lambda_F = 2\pi/k_F$; where k_F is the Fermi wave vector. For material like copper or gold, $\lambda_F = 0.5$ nm, and is much less than the free- electron- path Λ (Λ_{Cu}> 14 nm). If the system dimensions are less than a free-electron-path, the impurity scattering is negligible and the electron transport is regarded as ballistic (Mahboobeh, 2013).

This paper is organized as follows: Section II gives the background theory of M-S rectifying junctions, which are the ideal and non-ideal. Here the parametric quantities have effects as results deduced from the exact solution of M-S equilibrium junction equation on the effective Schottky barrier height, ESBH. Section III discusses the interface layer thickness effect on the carrier transport characteristics of the Al-GaN junction. Section IV, gives the results and discussion and lastly Section V, the conclusion.

2. Theory of M-S Junction

For a Schottky junction, where a metal and semiconductor with different Fermi energy levels are brought into contact, the Fermi energy will line up to a common level (under equilibrium). In the case of n-type semiconductor, which is of interest here, the Fermi energy is usually greater or higher than that of metal when laterally arranged. Because there are many empty states in the metal, electrons with sufficient energy flow into the metal from the semiconductor. By leaving the semiconductor, there will be empty or unfilled energy states left in the semiconductor. Furthermore, because the contact between the two different materials can never be ideal, the presence of chemical defects or broken (dangling) bonds will cause large number of unfilled surface states (Leonard and Yichen, 2011).

Disregarding the influence of surface states, the electrical properties of metal-semiconductor contact are determined by the work function of the metal and the electron affinity, χ of the semiconductor (Mehta and Mehta, 2009); and Ben and Sanjay, 2016). If the metal work function, ϕ_m is greater than semiconductor electron affinity, χ_s, discussion is confined to depletion contacts properties. The energetic properties of such levels are schematically depicted in Figure 1.

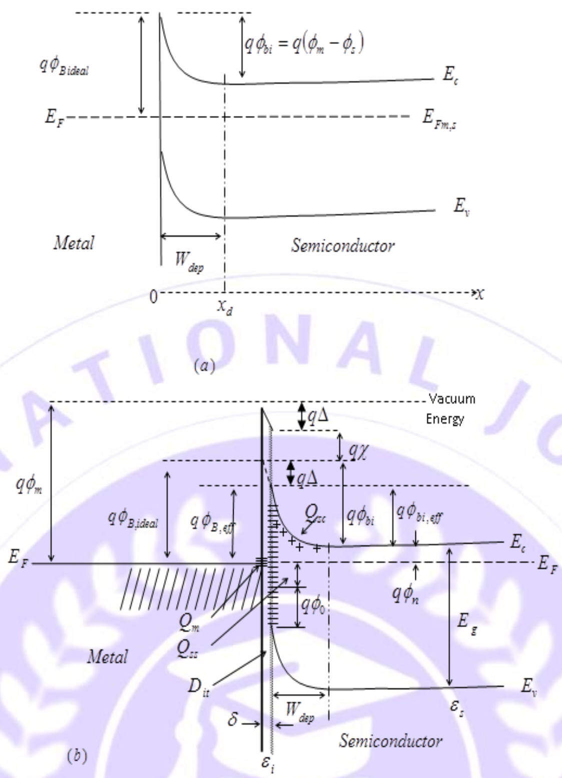

Figure.1. Metal and n-type Semiconductor contact: (a) ideal junction and (b) Non-ideal junction by (Sze and Kwok, 2007).

In Figure.2, the following are symbols' definitions:

ϕ_m - Metal work function (eV)

$\phi_{B,eff}$ - Effective barrier height of M-S junction (eV)

$\phi_{B,ideal}$ - Ideal barrier height at zero electric field (eV)

ϕ_0 - Neutral level (above E_V) of surface states (eV)

ϕ_n - Potential difference at the edge of depletion region (eV)

Δ - Potential across the interfacial layer (eV)

χ - Electron affinity of semiconductor, (From E_C to Vacuum, E_o), (eV)

ϕ_s - Semiconductor work function, (From E_{Fs} to Vacuum, E_{o}), (eV)

ϕ_{bi} - Built in junction potential at equilibrium (eV)

$\phi_{bi,eff}$ - Effective built in junction potential at equilibrium (eV)

ε_s - Permittivity of semiconductor (F/m)

ε_i - Permittivity of interfacial layer (F/m)

δ -Thickness of interfacial layer (nm)

Q_{sc} - Space charge density in semiconductor (C/cm^2)

Q_{ss} - Surface states charge density on semiconductor (C/cm^2)

Q_m - Surface charge density on metal (C/cm^2)

D_{it} - Density of interface states (cm^{-2}-eV^{-1})

W_{dep} -Width of depletion (nm)

In Figure (1*a*), the equilibrium potential or built-in potential, ϕ_{bi}, which prevents, further net electron diffusion from the semiconductor into the metal is expressed as the difference in work functions potential of the metal and semiconductor, (ϕ_m - ϕ_s). The potential barrier height, ϕ_B for electron injection from metal into the semiconductor conduction band is (ϕ_m - χ). The equilibrium potential can thus be decreased or increased by the application of either forward or reverse biased voltage.

At formation of an ideal contact, electrons are depleted from the semiconductor; a net positive charge is created in the semiconductor at the junction. An equilibrium is established when these charges are equal. It is within this region, called the depletion region, that all of the junction's electrical properties are established. The amount of band bending is called the built-in potential, ϕ_{bi}. For an electron to cross from the semiconductor to the metal, it must overcome ϕ_{bi}, and $\phi_{B,ideal}$. If the metal is held at a constant potential and a negative voltage applied to the n-type semiconductor, the Schottky barrier (built-in potential) is reduced, hence forward biased.

In the non-ideal contact Figure. (1*b*), an interfacial layer of thickness δ lies between the metal and the semiconductor, and accommodates a voltage drop, Δ. Now, let the interface-trap charge density D_{it} be states/cm^2/eV and be constant over the energy range from $q\phi_0$ + E_V to the Fermi level. For a metal in contact with n-type semiconductor, the surface states charge density on the semiconductor, Q_{ss} is therefore negative and is given by (Sze, 2009), in equation (2)

$$Q_{ss} = -qD_{it}\left(E_F - q\phi_0 + E_V\right) = -qD_{it}\left(E_g - q\phi_0\right) - q\phi_{B_n} \tag{2}$$

and the space charge density, Q_{sc} (Calahorra and Ritter, 2013), equation (3)

$$Q_{sc} = qN_D W_{dep} = \sqrt{2q\varepsilon_s N_D}\left(\phi_{B_n} - \phi_n - \frac{k_B T}{q}\right) \tag{3}$$

where ϕ_n is the potential at the edge of depletion width, and this is constant through the semiconductor and ϕ_{B_n} is the barrier height for metal in contact with an n-type semiconductor, N_D is the doping concentration, W_{dep} is the width of depletion and k_B the Boltzmann constant.

The total equivalent surface charge density on the semiconductor is the sum of equations (2) and (3) in the absence of space charge that could cause Schottky effects in the interfacial layer, and exactly equal and opposite to the surface charge on the metal. Therefore, the surface charge in the metal is as expressed by equation (4).

$$Q_m = -(Q_{ss} + Q_{sc}) \tag{4}$$

The interface potential drop, Δ across the interfacial layer is obtained by the application of Gauss's law (ϕ = $\bar{\boldsymbol{E}}\Phi \mathrm{d}\boldsymbol{A}$ = q_{enc}/ε) to the surface charge on the metal and semiconductor, equation (5)

$$\Delta = -\frac{\delta Q_m}{\varepsilon_i} \tag{5}$$

Equally, by inspection of the energy band diagram (Figure 2), we observed that equation (5) can be written as

$$\Delta = \phi_m - (\chi + \phi_{B_n}) \tag{6}$$

Eq. (6) results only and only if the Fermi energy level E_F is constant throughout the system at thermal equilibrium (Sze and Kwok, 2007).

The interface potential drop, Δ is eliminated from equations (5) and (6) and substituting for Q_m using equation (4), we obtain equation (7) (Sze and Kwok, 2007)

$$\phi_m - \chi - \phi_{Bn0} = \sqrt{\frac{2q\varepsilon_s N_D \delta^2}{\varepsilon_i^2}\left(\phi_{Bn0} - \phi_n - \frac{k_B T}{q}\right)} - \frac{q^2 D_{it}\delta}{\varepsilon_i}\left(\frac{E_g}{q} - \phi_0 - \phi_{Bn0}\right) \tag{7}$$

We call eqn. (7) the equilibrium state equation for metal-semiconductor interface junction. With some perseverance, we obtained an exact solution of eqn (7), so that $\phi_{Bn,0} \equiv \phi_{Bn,eff}$ is a function of ϕ_m. That is, the exact solution for the SBH is now the effective Schottky barrier height (ESBH) for the non-ideal junction. Having a quadratic solution, the real part was considered: (See Appendix **A**).

$$\phi_{Bn,eff} = \frac{(2a_3a_4 + a_1)}{2a_3^2} \pm \frac{1}{2a_3^2}\left[a_1^2 + 4(a_1a_3a_4 + a_3^2a_4^2) - 4(a_3^2a_4^2 + a_1a_3^2(\phi_n - \frac{k_BT}{q}))\right]^{1/2} \tag{8}$$

where $a_1 = \dfrac{2q\,\varepsilon_s\,N_D\,\delta^2}{\varepsilon_i^2}$, $a_2 = \dfrac{qD_{it}\,\delta}{\varepsilon_i}$, $a_3 = (1 + a_2) = \left(1 + \dfrac{qD_{it}\,\delta}{\varepsilon_i}\right)$, $a_4 = \phi_m - \chi + a_2(E_g - q\phi_0)$

During doping, to avoid pushing the semiconductor to a degenerate state, the doping function, $(E_C - E_F) \equiv \phi_n = \{E_g/2 - k_BT\ln(N_D/n_i)\} > k_BT$ was ensured, where n_i is the intrinsic carrier concentration of the semiconductor. To use eqn (8), the model parameters that, are relevant, are as given in Table 1.

Table 1: Defined Interface Model Parameters and Temperature

Interface states density, D_{it}, ($cm^{-2}eV^{-1}$)	Interface layer thickness, δ, (nm)	Interface permittivity, ε_i, (Fm^{-1})	Neutral energy level, $q\phi_0$ (eV)	Temperature, (K)
10^{10}	0.5	1.5 ε_0	0.25	300
10^{12}	1.0	2.0ε_0	0.75	330
10^{14}	1.5	2.5ε_0	1.25	360
10^{16}	2.0	3.0ε_0	1.75	390
10^{18}	2.5	3.5ε_0	2.25	420

3. Effect of Junction Interface Layer Thickness on Carrier Transport Characteristics

The ideality factor η is a measure that corrects the deviation from the thermionic emission of current transport characteristics in M-S junctions. It accounts for the defects causing the non-thermionic in the current transport. The factors subdue the effects or influence the thermionic field emission (TFE), the field emission (FE), and then the generation and recombination (GR),in the M-S interface. In the presence of interfacial layer, such as oxide, the current density will be reduced in a metal-semiconductor contact with interfacial layer thickness when it is considered. The forward bias current density, J in the Schottky junction is no longer due to thermionic emission purely and therefore is corrected by a tunneling factor and this factor accounts for the suppression of the current due to tunneling introduced in the reverse saturation current density, J_s, of M-S junction given by (Hudait, and Krupanidhi, 2000; and Saroj, 2012) as

.

$$J = J_s\left[\exp\left(\frac{qV_D}{\eta k_B T}\right) - 1\right] \tag{9}$$

and

$$J_s = \overset{*}{A}T^2 \varphi_t \exp(-\frac{q\phi_{Bn}}{k_B T}) \tag{10}$$

where A^* is the effective Richardson constant, q is charge of the electron, k_B is the Boltzmann constant and φ_t is the transmission coefficient across the interfacial layer given by

$$\varphi_t = \exp(4\pi / h)(2m^*)^{1/2} = \exp(-\alpha_T \xi^{1/2} \delta) \tag{10A}$$

α_T (in eV$^{-0.5}$Å^{-1}) is a constant, $\xi^{1/2}$ (in eV) and δ (in Å) are the effective mean tunneling barrier height by the thin interfacial layer or energy difference between the conduction band edge of the semiconductor and that of the interfacial layer thickness of the oxide layer. The junction transport equation can then now be written as

$$J = A^* T^2 \exp\left(-\alpha_T \xi^{1/2} \delta\right) \exp\left(\frac{-q\phi_B}{k_B T}\right)\left[\exp\left(\frac{qV}{\eta k_B T}\right) - 1\right] \tag{11}$$

The constant, αT = $2(2qm^*)^{1/2}/\hbar \approx 1.01$ eV$^{-0.5}$Å^{-1} approaches unity when the effective mass, m^* of the electron in the insulator is equal to the free electron mass. Hence, equation (11) becomes

$$J = A^* T^2 \exp\left(-\xi^{1/2} \delta\right) \exp\left(\frac{-q\phi_B}{k_B T}\right)\left[\exp\left(\frac{qV_D}{\eta k_B T}\right) - 1\right] \tag{12}$$

This can as well be written as

$$I = a_i A^* T_i^2 \exp\left(-\xi^{1/2} \delta\right) \exp\left(\frac{-q\phi_B}{k_B T_i}\right)\left[\exp\left(\frac{qV_D}{\eta k_B T_i}\right) - 1\right] \tag{13}$$

where a_i is the M-S surface contact area of the junction.

4. Results and Discussion

The effective Richardson constant for n-GaN semiconductor, ~ 26.4×10^4 Am^{-2}K^{-2} and the ideality factor, η = 11.9, been the least experimental value for axial nanowire Al-GaN contact (Chanoh, H., 2008), was used whilst neglecting the Ohmic contact potential drop. Simulation of the current-voltage characteristics with defined mean tunneling barrier height, ξ = 0.09, interface thickness, δ = 1.5, 2.0, 2.5 and 3.0 nm and metal-semiconductor surface contact area of 2.251×10^{-16} m^2 shows a suppressed effect on both the forward and reverse bias of the *I-V* characteristics, Figure (2a). This is the same for all other surface contact areas of the junction device at nanowire scale. The radii of the semiconductor nanowire and the interfacial layer thickness have also been observed to pose no significant effect on the analytical characteristics of the metal-wrapped semiconductor Shottky junction. However, for the temperature, this can be seen how the curve shifts about the axes origin with temperature variation, Figure (2b).This indicates that the ideality factor, η decreases as temperature increases.

The interface parameters (the interface states density, interface permittivity, neutral surface states, interface layer thickness) and temperature, as model parameters are given in Table 1. These are model parameters used in the analysis on the barrier height of the metal-semiconductor junction. The results obtained for the varied doping densities, interface states, interface permittivity, neutral surface states are as presented in Tables 2, 3, 4, 5, and 6. The effective Schottky barrier height, ESBH was found to decrease with increase in doping density for the defined interfacial layer parameters at a given temperature and increases with temperature for any given doping density. The effective barrier height could be seen to increase with temperature almost linearly by ~5.171×10^{-3} eV with increase in temperature from 300 K to 420 K and this may be associated with the avalanched charge energy gain by carriers with temperature as being transported across the barrier height.

The interface layer thickness, ($\delta = R_{Me} - R_{NW}$), effect, on the carrier transport characteristics, Figure (2b), was very insignificant as the curves, Figure 2a, are distinctly inseparable in the range of 1.5 nm to 3.0 nm with the doping functions. Therefore, we can confidently conclude that the thickness of the interface layer in between the metal and the semiconducting nanowire in the given range has no effect on the carrier transport characteristics, in the nano scale ranges.

The results of the interfacial parameters effects on ESBH`using the exact solution, given by eqn (8), are as presented in Tables 2, 3, 4, 5 and 6. We expect imaginary result in the computations but none has been obtained.

Table 2: Interface States Density effect on ESBH at room Temperature (300 K) with varied N_D , ε_i=1.5ε_0, δ =1.5 nm and $q\phi_0$ =0.25 eV

D_{it} State s/cm^3/eV	N_{D1} 10^{16} cm^{-3}	N_{D2} 2×10^{16} cm^{-3}	N_{D3} 10^{17} cm^{-3}	N_{D4} 2×10^{17} cm^{-3}	N_{D5} 10^{18} cm^{-3}	N_{D6} 2×10^{18} cm^{-3}
	$\phi_{Bn,eff}$ (eV)	$\phi_{Bn,eff}$ (eV)	$\phi_{Bn,eff}$ (eV)	$\phi_{Bn,ff}$ (eV)	$\phi_{Bn,eff}$ (eV)	$\phi_{Bn,eff}$ (eV)
10^{10}	0.194646	0.176725	0.135115	0.0117194	0.0755837	0.0576631
10^{12}	0.194646	0.176725	0.135115	0.0117194	0.0755837	0.0576631
10^{14}	0.194646	0.176725	0.135115	0.0117194	0.0755837	0.0576631
10^{16}	0.194646	0.176725	0.135115	0.0117194	0.0755837	0.0576631
10^{18}	0.194646	0.176725	0.135115	0.0117194	0.0755837	0.0576631

The results in Table 2 indicate that for varied interface states density and a given carrier concentration, the ESBH remains constant but decreases with increase in doping density.

Table 3: Interface Layer Thickness Effect on ESBH at room Temperature (300K) with varied N_D , D_{it}=2×10^{12} states/cm^2/eV, ε_i=1.5ε_0, and $q\phi_0$ =0.25 eV

δ (in nm)	N_{D1} 10^{16} cm^{-3}	N_{D2} 2×10^{16} cm^{-3}	N_{D3} 10^{17} cm^{-3}	N_{D4} 2×10^{17} cm^{-3}	N_{D5} 10^{18} cm^{-3}	N_{D6} 2×10^{18} cm^{-3}
	$\phi_{Bn,eff}$ (eV)	$\phi_{Bn,eff}$ (eV)	$\phi_{Bn,eff}$ (eV)	$\phi_{Bn,eff}$ (eV)	$\phi_{Bn,eff}$ (eV)	$\phi_{Bn,eff}$ (eV)
0.5	0.194646	0.176725	0.135115	0.117194	0.0755837	0.0576631
1.0	0.194646	0.176725	0.135115	0.117194	0.0755837	0.0576631
1.5	0.194646	0.176725	0.135115	0.117194	0.0755837	0.0576631
2.0	0.194646	0.176725	0.135115	0.117194	0.0755837	0.0576631
2.5	0.194646	0.176725	0.135115	0.117194	0.0755837	0.0576631

Results of Table 3 indicate that interface layer thickness, δ has no effect on ESBH as long as the doping density is constant. However, for any given inertfacial layer thickness, SBH decreases with increase in the doping density.

Table 4: Interface Permittivity Effect on ESBH at room Temperature (300 K) with varied N_D, δ =0.5 nm, D_{it}=10^{12}states/cm^2/eV and $q\phi_0$ =0.25 eV

ε_i	N_{D1} 10^{16} cm^{-3}	N_{D2} 2×10^{16} cm^{-3}	N_{D3} 10^{17} cm^{-3}	N_{D4} 2×10^{17} cm^{-3}	N_{D5} 10^{18} cm^{-3}	N_{D6} 2×10^{18} cm^{-3}
	$\phi_{Bn,eff}\,(eV)$	$\phi_{Bn,eff}\,(eV)$	$\phi_{Bn,eff}\,(eV)$	$\phi_{Bn,eff}\,(eV)$	$\phi_{Bn,eff}\,(eV)$	$\phi_{Bn,eff}\,(eV)$
1.5ε_0	0.194646	0.176725	0.135115	0.117194	0.0755837	0.0576631
2.0ε_0	0.194646	0.176725	0.135115	0.117194	0.0755837	0.0576631
2.5ε_0	0.194646	0.176725	0.135115	0.117194	0.0755837	0.0576631
3.0ε_0	0.194646	0.176725	0.135115	0.117194	0.0755837	0.0576631

Interface permittivity presents no effect on ESBH except when there is an increase in doping density for any given interface permittivity

Table 5: Neutral Surface States Effect on ESBH at room Temperature (300 K) with varied N_D, δ =0.5 nm, D_{it}=10^{12} states/cm^2/eV and ε_i=1.5ε_0.

$q\phi_0$ (eV)	N_{D1} 10^{16} cm^{-3}	N_{D2} 2×10^{16} cm^{-3}	N_{D3} 10^{17} cm^{-3}	N_{D4} 2×10^{17} cm^{-3}	N_{D5} 10^{18} cm^{-3}	N_{D6} 2×10^{18} cm^{-3}
	$\phi_{Bn,eff}\,(eV)$	$\phi_{Bn,eff}\,(eV)$	$\phi_{Bn,eff}\,(eV)$	$\phi_{Bn,eff}\,(eV)$	$\phi_{Bn,eff}\,(eV)$	$\phi_{Bn,eff}\,(eV)$
0.25	0.194646	0.176725	0.135115	0.117194	0.0755837	0.0576631
0.75	0.194646	0.176725	0.135115	0.117194	0.0755837	0.0576631
1.25	0.194646	0.176725	0.135115	0.117194	0.0755837	0.0576631
1.75	0.194646	0.176725	0.135115	0.117194	0.0755837	0.0576631
2.25	0.194646	0.176725	0.135115	0.117194	0.0755837	0.0576631

Neutral surface states have no effect on ESBH. However, for a given neutral surface states value, $q\phi_0$, the ESBH also decreases with increase in the doping density.

Table 6: Temperature Effect on ESBH with varied N_D, ε_i=1.5ε_0, δ =1.5 nm, D_{it} =10^{12} states(cm^{-2}eV^{-1}) and $q\phi_0$ =0.25 eV

T (K)	N_{D1} 10^{16} cm^{-3}	N_{D2} 2×10^{16} cm^{-3}	N_{D3} 10^{17} cm^{-3}	N_{D4} 2×10^{17} cm^{-3}	N_{D5} 10^{18} cm^{-3}	N_{D6} 2×10^{18} cm^{-3}
	$\phi_{Bn,eff}\ (eV)$	$\phi_{Bn,eff}\ (eV)$	$\phi_{Bn,eff}\ (eV)$	$\phi_{Bn,eff}\ (eV)$	$\phi_{Bn,eff}\ (eV)$	$\phi_{Bn,eff}\ (eV)$
300	0.194646	0.176725	0.135115	0.117194	0.117194	0.117194
330	0.195939	0.178018	0.136408	0.1184871	0.1184871	0.1184871
360	0.197231	0.179310	0.137700	0.119779	0.119779	0.119779
390	0.198524	0.180603	0.138993	0.121072	0.121072	0.121072
420	0.199817	0.181896	0.140286	0.122365	0.122365	0.122365

The effective Schottky barrier height, ESBH was found to be affected by temperature. It decreases with increase in doping density for defined interfacial layer parameters at a given temperature and inecreases with temperature for any given range of doping density, as could be seen in Table 6. The effective barrier height could be seen to increase with temperature almost linearly by ~5.171×10^{-3}eV with increase in temperature from 300 to 420 K and this may be associated with the increase in energy acquired by charge carriers to be transported across the barrierheight. The lowest value of the Schottky barrier height obtained can be ascribed to an enhanced electric field at the depletion region and size of the nano Schottky junction. Still referring to Table 6, from doping densities, N_{D4} to N_{D6}, a phenomenon of saturation is observed, which connotes degeneracy in the nanoscale.

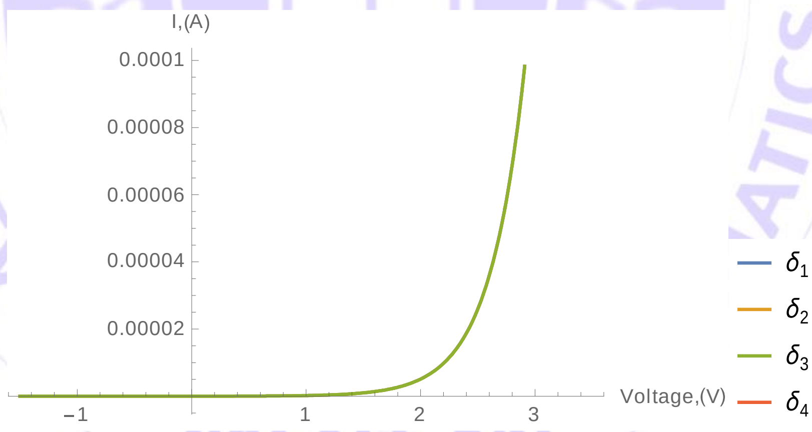

(***a***)

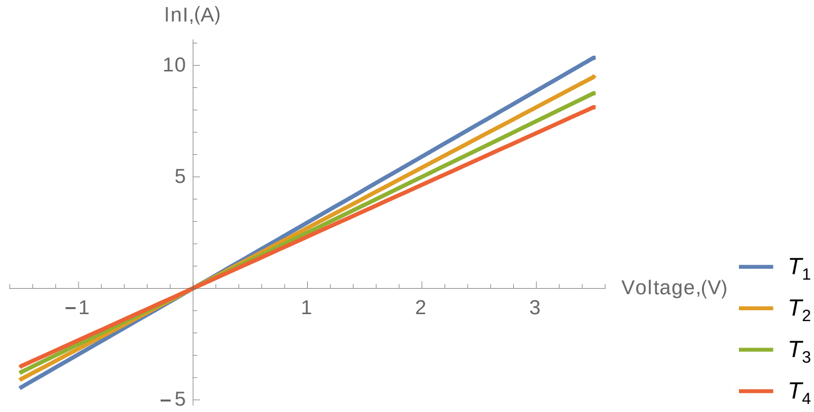

(***b***)

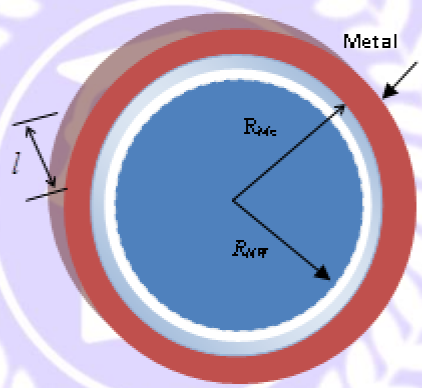

(***c***)

Figure 2 (a) Forward and reverse bias current-voltage characteristics of Al-GaN nanowire with varied interfacial layer thickness, δ, (b) Analytical characteristic curves of metal-wrapped nanowire Schottky junction and (c) Metal-Wrapped (Al-GaN) semiconductor Schottky junction; R_{Me} is the metal radius, R_{NW} is the semiconductor radius and l is height of the cylindrical structure

5. Conclusion

This paper analysed the impact of interface parametric quantities, IPQ, doping density and temperature on Schottky barrier height and the interface layer thickness, ILT on carrier transport characteristic curves of a metal-wrapped semiconductor nanowire Schottky junction quantitatively. The effective Schottky barrier height dependence on doping function and temperature were found to be in agreement with that of the axial structures (Saroj, 2012) except for extremely high dopping densities as presented in Table 6. And, from the defined IPQ model parameters, this has shown no significant effects on the Schottky barrier height of a nanoscale metal-semiconductor junction. Similarly, the ILT effect on the carrier transport characteristics of the geometrical structure is insignificant.

References

Ben, G. S. and Sanjay K. B. (2016). Solid state electronic devices (7th edn); Pearson prentice Hall, USA.

Calahorra,Y. and Ritter, D. (2013). Surface depletion effects in semiconducting nanowires Having a non- radial doping profile. *Journal of Applied Physics* 114(12): 12 14 10

Chanoh,H.,Jung-Hwan.,Seung-Yong,L.,Chan-Oh, J.,Tae-Hong, K., Pyung, C., and Sang-Kwom, L. (2008). The formation and characterization of electrical contacts (Schottky and Ohmic) on Gallium nitride nanowire. *Journal of Physics D: Applied Physics*. **41**105103

Das, S. N., Sarangi S., Sahu S. N., Pal, A. K. (2009). Metal Contacts in nanocrystalline n-type GaNschottky diodes. *Journal of nanoscience and nanotechnology* Vol.9, 2532-2539

Guven C. and Nazim U.(2004). Schottky barrier height dependence on metal work function for p-type Si Schottky diodes Z. *Naturforsch*. **59a,** 795-798

Hudait, M. K., and Krupanidhi, S. B. (2000). Effects of thin oxide in metal-semiconductor and metal- insulator-semiconductor epi-GaAsschottky diodes. Pergamon, *Solid-State Electronics,*1089-1097

James, D. P., and Bernard, C. B. (2007). Solid State Physics. Introduction to the theory. Springer (India) Private Ltd. pp 620-639.

Mahboobeh, S. M. (2013). Calculating the electrical conductivity of metal nanoiwires. International Research Journal of Applied and Basic Sciences. Vol. 5(11): 1353-1362.

Mehta V. K. and Mehta Shahu (2009). Introduction to solid state Physics (7th ed). John Willey and Sons Inc. India.

Leonard, J. B. and Yichen L. (2011). ZnO Schottky barrier contacts. Journal of Applied Physics. 109, 121301

Rhodrick E. H.(1978). *Metal semiconductor contacts*. Oxford University, Oxford.

Rhodrick, E. H., Frensley, W. R., and Shan, M. P. (1993). Hand bookon semiconductors, properties of junctions and Barriers. Elsevier Science publication. Vol. 4, pp 1-96**.**

Saroj, B. (2012). The role of interface state density in I-V characteristics of metal-s emiconductor contact with interfacial layer. *International Journal of Emerging Technology and advance Engineering.* Vol. 2, **12** pp 364-366

Sze S. M. and Kwok K N G. (2007). Physics of Semiconductor Devices, 3rd ed.John Wiley and Sons, INC, Publication, New Jessy, Canada. pp 144

Sze, S. M. (2009). Semiconductor Devices, revised edition. John Wiley and Sons Inc, India

Tolley, R., Silvidik, A., Little, C., Eid, F. K. (2013). Conductance Quantization: A Laboratory experiment in a senior Level nanoscale science and Technology course. *American Journal of Physics*.81 (4); doi: 10.119/1.4765331.

Wolf E. L. (2004). *Nanophysics and Nanotechnology*: *An introduction tomodern concepts in nanoscience.* Wiley-VCH: Weinheim, Germany

Zettil Nouredine (2009). Quantum Mechanics, Concepts and Applications,2nd edn. Chichester: Willey. p365

APPENDIX A

The zero biased SBH, $\phi_{B_{no}}$ in equation (7), is replaced with, the effective barrier height, $\phi_{B_{n,eff}}$, in the presence of ILT and solved as follows and results used in the computations.

$$\phi_m - \chi - \phi_{B_{n,eff}} = \left[\frac{2q\varepsilon_s N_D \delta^2}{\varepsilon_i^2} \left(\phi_{B_{n,eff}} - \phi_n - \frac{k_B T}{q} \right) \right]^{1/2} - \frac{qD_{it}\delta}{\varepsilon_i} \left(E_g - q\phi_0 - \phi_{B_{n,eff}} \right) \tag{A.1}$$

Let $a_1 = \dfrac{2q\varepsilon_s N_D \delta^2}{\varepsilon_i^2}$ and $a_2 = \dfrac{qD_{it}\delta}{\varepsilon_i}$

Using a_1 and a_2 in eq. (A.1), get

$$\phi_m - \chi - \phi_{B_{n,eff}} = \left[a_1 \left(\phi_{B_{n,eff}} - \phi_n - \frac{k_B T}{q} \right) \right]^{1/2} - a_2 \left(E_g - q\phi_0 - \phi_{B_{n,eff}} \right) \tag{A.2}$$

Eq. (A.2) can be written as

$$-\phi_{B_{n,eff}} (1 + a_2) + \phi_m - \chi + a_2 (E_g - q\phi_0) = \left[a_1 \left(\phi_{B_{n,eff}} - \phi_n - \frac{k_B T}{q} \right) \right]^{1/2} \tag{A.3}$$

From eq. (A.3) define

$$a_3 = (1 + a_2) \tag{A.4}$$

$$a_4 = \phi_m - \chi + a_2 (E_g - q\phi_0) \tag{A.5}$$

Using eq. (A.4) and (A.5) in (A.3) gives

$$-a_3 \phi_{B_{n,eff}} + a_4 = \left[a_1 \left(\phi_{B_{n,eff}} - \phi_n - \frac{k_B T}{q} \right) \right]^{1/2} \tag{A.6}$$

Squaring both sides of eq. (A.6) gives

$$a_3^2 \phi_{B_{n,eff}}^2 - (2a_3 a_4 + a_1) \phi_{B_{n,eff}} + a_4^2 + a_1 (\phi_n + \frac{k_B T}{q}) = 0 \tag{A.7}$$

In eq. (A.7), we define the followings:

$$a = a_3^2 \tag{A.8a}$$

$$b = -(2a_3 a_4 + a_1) \tag{A.8b}$$

$$c = a_4^2 + a_1 (\phi_n + \frac{k_B T}{q}) \tag{A.8c}$$

Using eqs. (A.8a), (A.8b) and (A.8c) in eq. (A.7) gives

$$a\phi_{B_{n,eff}}^2 + b\phi_{B_{n,eff}} + c = 0 \tag{A.9}$$

Eq. (A.9) is quadratic in $\phi_{Bn,eff}$. Thus $\phi_{Bn,eff}$ is

$$\phi_{B_{n,eff}} = \frac{-b}{2a} \pm \frac{1}{2a}\left(b^2 - 4ac\right)^{1/2} \tag{A.10}$$

From eq. (A.8a-c), we obtained

$$b^2 = 4a_3^2 a_4^2 + 4a_1 a_3 a_4 + a_1^2 \tag{A.11}$$

$$ac = a_3^2 a_4^2 + a_1 a_3^2 (\phi_n + \frac{k_B T}{q}) \tag{A.12}$$

Using eq. (A.11) and (A.12) in eq. (A.10) gives

$$\phi_{B_{n,eff}} = \frac{\left(2a_3 a_4 + a_1\right)}{2a_3^2} \pm \frac{1}{2a_3^2}\left[a_1^2 + 4(a_1 a_3 a_4 + a_3^2 a_4^2) - 4(a_3^2 a_4^2 + a_1 a_3^2 (\phi_n - \frac{k_B T}{q}))\right]^{1/2} \tag{A.13}$$

Recall: $a_1 = \frac{2q\varepsilon_s N_D \delta^2}{\varepsilon_i^2}$, $a_2 = \frac{qD_{it}\delta}{\varepsilon_i}$, $a_3 = \left(1 + a_2\right) = \left(1 + \frac{qD_{it}\delta}{\varepsilon_i}\right)$

$$a_4 = \phi_m - \chi + a_2\left(E_g - q\phi_0\right)$$

Note, when $\delta = 0,\ \varepsilon_i = 0$; $a_1 = 0,\ a_2 = 0,\ a_3 = 1,\ and\ a_4 = \phi_m - \chi$. Substituting these into (A.13) above, we obtain $\phi_{B_n} = \phi_m - \chi$, which is the barrier height for an ideal metal-semiconductor junction